

Au@Gd Core-Shell Nanoparticles as a CT/MR Bimodal Contrast Agent

Min-Kyoung Kang¹, Hee-Kyung Kim¹, Ki-Hye Jung², Ji-Ae Park³, Seung-Tae Woo⁴, Joo-Hyun Kim⁴, Eun-Young Jeon⁵, Tae-Jeong Kim^{*2}, and Yongmin Chang^{*1,6}
¹Medical & Biological Engineering, Kyungpook National University, Daegu, Korea, ²Applied Chemistry, Kyungpook National University, Daegu, Korea, ³Molecular Imaging Research Center, Korea Institute of Radiological & Medical Science, Seoul, Korea, ⁴Bayer Healthcare, Medical care, Seoul, Korea, ⁵The Advanced Medical Technology Cluster for Diagnosis & Prediction, Kyungpook National University, Daegu, Korea, ⁶Diagnostic Radiology and Molecular Medicine, Kyungpook National University, Daegu, Korea

Introduction

The development of contrast agents for use across multiple imaging modalities such as PET/MRI, PET/CT, SPECT/CT, and CT/MRI is a versatile area of research gaining a lot of interest in recent times. X-ray computed tomography (CT) has been one of the most widely used imaging modalities in hospitals in terms of frequency of the use and cost. Current contrast for CT is mostly based on iodinated small molecules which are effective in absorbing X-rays. However, one of the serious shortcomings of iodinated contrast agents is that they reveal very short imaging time due to rapid clearance by the kidney. In contrast, gold nanoparticles (AuNPs) possess a much higher X-ray absorption coefficient than iodine (5.16 and 1.94 cm²/g, respectively, at 100 keV). In addition, AuNPs possess many attractive features such as a very high surface-to-volume ratio, high stability, size tunability, and biocompatibility which may enable AuNPs to be a good substitute for iodine-based CT agents. Although there are now known a myriad of low-molecular Gd-chelate based MRI contrast agents (CAs), gadolinium nanoparticles (GdNPs) may represent a new and different approach to the development of novel MRI CAs such as blood-pool contrast agents (BPCAs) or organ/tumor targeting MRI CAs. Recent interest in such GdNPs-based CAs may be found in their ability to act as a R₁ agent as well as their relationship to currently employed Gd-chelates. Therefore, GdNPs, when properly modified, would in principle provide a new entry into highly versatile MRI CAs with multifunctionality. Herein, we present Au@Gd core-shell nanoparticle formulated as Au@SiO₂@Gd@PEG as a potential candidate for a new class of CT/MR bimodal contrast agents.

Material and Methods

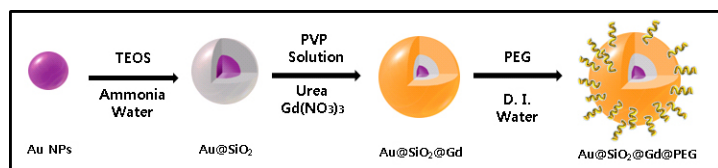
All reagents were purchased from commercial sources and used as received. AuNPs and Au@SiO₂ were prepared according to the literature method. Au@SiO₂@Gd@PEG nanoparticles prepared as illustrated in Scheme 1. Microanalysis was performed by Center for Instrumental Analysis, KNU. CT (X-ray computed tomography) was performed using a multidetector CT system with 400 μA and 70 kVp. T₁ measurements were carried out using an inversion recovery method with a variable inversion time at 1.5 Tesla (64 MHz) MR unit (GE Healthcare, Milwaukee, WI, USA) at 293 K. The MR images were acquired at 35 different T₁ values ranging from 50 to 1750 ms. T₁ relaxation times were obtained from the non-linear least squares fit of the signal intensity measured at each T₁ value. For T₂ measurements, the CPMG (Carr-Purcell-Meiboom-Gill) pulse sequence was adapted for multiple spin-echo measurements. Thirty four images were acquired with 34 different echo time (TE) values ranging from 10 to 1900 ms. T₂ relaxation times were obtained from the non-linear least squares fit of the mean pixel values for the multiple spin-echo measurements at each echo time. Relaxivities (R₁ and R₂) were then calculated as an inverse of the relaxation time per mM. The determined relaxation times (T₁ and T₂) and relaxivities (R₁ and R₂) were finally image-processed to give the relaxation time map and relaxivity map, respectively.

Results and Discussion

The Au@Gd core shell nanoparticles were prepared as a new class of CT/MR bimodal CAs (cf. Scheme 1). To examine the feasibility of Au@SiO₂@Gd@PEG as a CT/MR bimodal imaging probe, we carried out X-ray absorption and MRI phantom studies. Au@SiO₂@Gd@PEG exhibits R₁ relaxivity (= 13.01 mM⁻¹ s⁻¹) four to five times as high as that of Omniscan[®] (cf. Table 1). R₁ and R₂ maps and plots of R₁ and R₂ relaxivities of Au@SiO₂@Gd@PEG show as functions of the gadolinium concentration (cf. Figure 1). The R₁ and R₂ maps become the brightest at the gadolinium concentration of 1 mM, and Au@SiO₂@Gd@PEG exhibits brighter image than Ultravist[®] and Omniscan[®] (cf. Figure 2). The CT image of Au@SiO₂@Gd@PEG is as expected to reveal the highest intensity among others including conventional iodine based CT probes in that the present system contains the gold core possessing strong X-ray absorption (cf. Figure 2).

Conclusions

The work describes the synthesis of core-shell nanoparticles Au@SiO₂@Gd@PEG and their potential application as a CT/MR bimodal imaging probe. The present system exhibits not only higher R₁ relaxivity but also higher X-ray attenuation than their commercial counterparts such as Ultravist[®] and Omniscan[®]. The R₁ relaxivity of Au@SiO₂@Gd@PEG is almost five times as high as that of Omniscan[®].



Scheme 1. Synthesis of Au@SiO₂@Gd@PEG: Au@citrate; Au@SiO₂; Au@SiO₂@Gd.

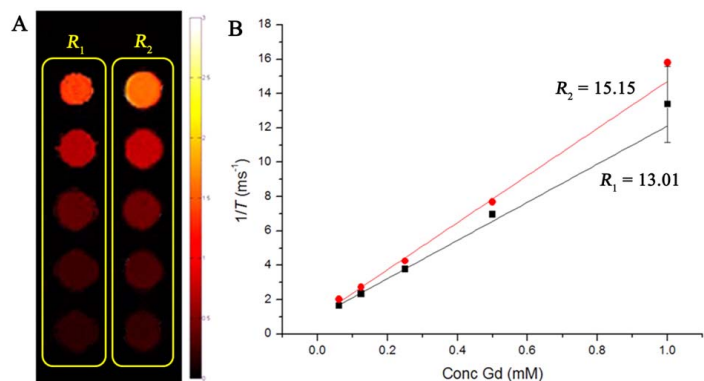


Figure 1. (A) R₁ and R₂ maps of Au@SiO₂@Gd@PEG and (B) linear plots of 1/T₁ and 1/T₂ as functions of [Gd] measured at 1.5 T and 293 K.

Table 1. Experimental relaxation times (mM⁻¹ s⁻¹) and relaxivities (mM⁻¹ s⁻¹) of Omniscan[®] and Au@SiO₂@Gd@PEG at the 1 mM concentrations and 293 K.

	T ₁	R ₁	T ₂	R ₂
Omniscan [®]	306.73	3.30	267.29	3.70
Au@SiO ₂ @Gd@PEG	70.93	13.38	63.25	15.51

Figure 2. CT phantom (70 kVp, 0.4 mA, 200 ms) images and HU (Hounsfield) scales of Au@SiO₂@Gd@PEG, Omniscan[®], and Ultravist[®].

		HU		HU	
	20 mM				
	20 mM 50 mM	Au@GdNPs	2972 ± 138	Ultravist [®] 1 M	3284 ± 184
	50 mM 100 mM	Omniscan [®] 500 mM	2307 ± 135	Ultravist [®] 500 mM	2326 ± 96
	100 mM 250 mM	Omniscan [®] 250 mM	1463 ± 97	Ultravist [®] 250 mM	1217 ± 75
	250 mM 500 mM	Omniscan [®] 100 mM	612 ± 77	Ultravist [®] 100 mM	563 ± 67
	500 mM	Omniscan [®] 50 mM	288 ± 67	Ultravist [®] 50 mM	269 ± 63
	582 mM	Omniscan [®] 20 mM	131 ± 71	Ultravist [®] 20 mM	130 ± 63